JOURNAL OF AIRCRAFT
Vol. 34, No. 1, January–February 1997

Development of a Low-Cost and Versatile Flight Test Platform

L. M. B. C. Campos,* A. A. Fonseca,† J. R. C. Azinheira,‡ and J. P. Loura§
Instituto Superior Tècnico, Lisbon 1096, Portugal

This paper describes the creation of an independent flight test facility in Portugal, based on international and national cooperation; the flying element is the basic aircraft for flight research (BAFR), a CASA 212 Aviocar twin-turboprop light transport, fitted with a flight test instrumentation (FTI) system, from which smaller dedicated FTIs were developed for several other aircraft. A part of one of the research projects carried out with BAFR, viz., a linear longitudinal stability model, including propeller slipstream effects is described. The model is reduced from 3 × 5 form to a 4 × 4 autonomous system of differential equations, from which the frequency and damping of the phugoid and short period modes are determined. The model parameters were identified from flight tests of selected maneuvers and the reconstruction of flight data using the model served to validate the latter.

Nomenclature

A_{ij} = 3 × 5 stability matrix in dimensional form, Eq. (14a)
$\boldsymbol{B}_i$ = three-dimensional control vector in dimensional form, Eq. (14b)
C_D, C_L = drag and lift coefficients
C_{ij} = 3 × 5 stability matrix in dimensionless form, Eqs. (24a) and (25)
c = mean aerodynamic chord
$\boldsymbol{D}_i$ = three-dimensional control vector in dimensionless form, Eq. (22)
$\boldsymbol{e}_x$, $\boldsymbol{e}_y$, $\boldsymbol{e}_z$ = unit vectors in x, y, and z directions
$\boldsymbol{F}$ = total force
f = Fourier spectrum, Eq. (44b)
$\boldsymbol{G}$ = gravity force
g = acceleration of gravity
H_{ij} = 4 × 4 stability matrix in autonomous system
$I_{x,y,z}$ = principal moments of inertia
j = dimensionless acceleration of gravity, Eq. (24b)
$\boldsymbol{L}$ = angular momentum
$\boldsymbol{M}$ = moment of forces
m = aircraft mass
$\boldsymbol{N}_i$ = four-dimensional control vector in autonomous system
P = power spectral density of input signal, Eq. (44a), deg
q = pitch rate
S = reference area
s = variable in Laplace transform
T = duration of pitch input, s
t = time
U = total longitudinal airspeed
U_0 = longitudinal airspeed in steady state
u = longitudinal airspeed perturbation
W = total normal airspeed
w = normal airspeed perturbation
$\boldsymbol{X}_j$ = vector of five independent dimensional variables, Eq. (2)
$\bar{\boldsymbol{X}}_j$ = vector of five independent dimensionless variables, Eq. (19)
x = longitudinal coordinate
$\boldsymbol{Y}_i$ = vector of three dependent dimensional variables, Eq. (1)
$\bar{\boldsymbol{Y}}_i$ = vector of three dependent dimensionless variables, Eq. (20)
y = transverse horizontal coordinate
$\boldsymbol{Z}_i$ = four-dimensional vector of autonomous system, Eq. (26)
$\tilde{Z}_i$ = Laplace transform of Z_i
Z_i' = time derivative of Z_i
z = transverse coordinate in vertical plane
α = angle of attack
δ_e = angle of deflection of elevator
δ_{ij} = identity matrix
θ = pitch angle
θ_0 = amplitude of pitch input
λ = decay time to half-amplitude
μ = reduced mass, Eq. (23a)
ν = reduced inertia, Eq. (23b)
ξ = damping ratio
ρ = mass density
τ = period
$X_{a,b,c}$ = quantity X for step, doublet, and 3211 input, respectively
X_{ph} = quantity X for phugoid mode
X_{sp} = quantity X for short-period mode
$\boldsymbol{\Omega}$ = angular velocity
ω = frequency, rad/s

Received Dec. 2, 1993; revision received Aug. 5, 1996; accepted for publication Sept. 3, 1996.

*Professor, Mechanical and Aerospace Engineering. Associate Fellow AIAA.
†Research Assistant, Aerospace Mechanics Section.
‡Assistant Professor, Department of Mechanical Engineering.
§M.S. Student, Department of Electrical Engineering.

I. Introduction

THE motivation for the creation of the independent flight test facility (IFTF) was to have, in Portugal, a flight test capability that could be used for basic research or practical applications, in a national or international context. Thus, international cooperation was both the beginning and purpose of the flight test facility. The international cooperation and national coordination are based on existing local engineering skills, which have to be honed in the field of flight testing, as part of the schedule of the program (Fig. 1). In fact, the program started with the generic training of Portuguese mechanical and electrical engineers in flight test techniques, done in one of the supporting nations. This was followed by specific training on the equipment to be transferred at another supporting nation. These engineers then coordinated the transfer of the flight test instrumentation to Portugal, its checking on

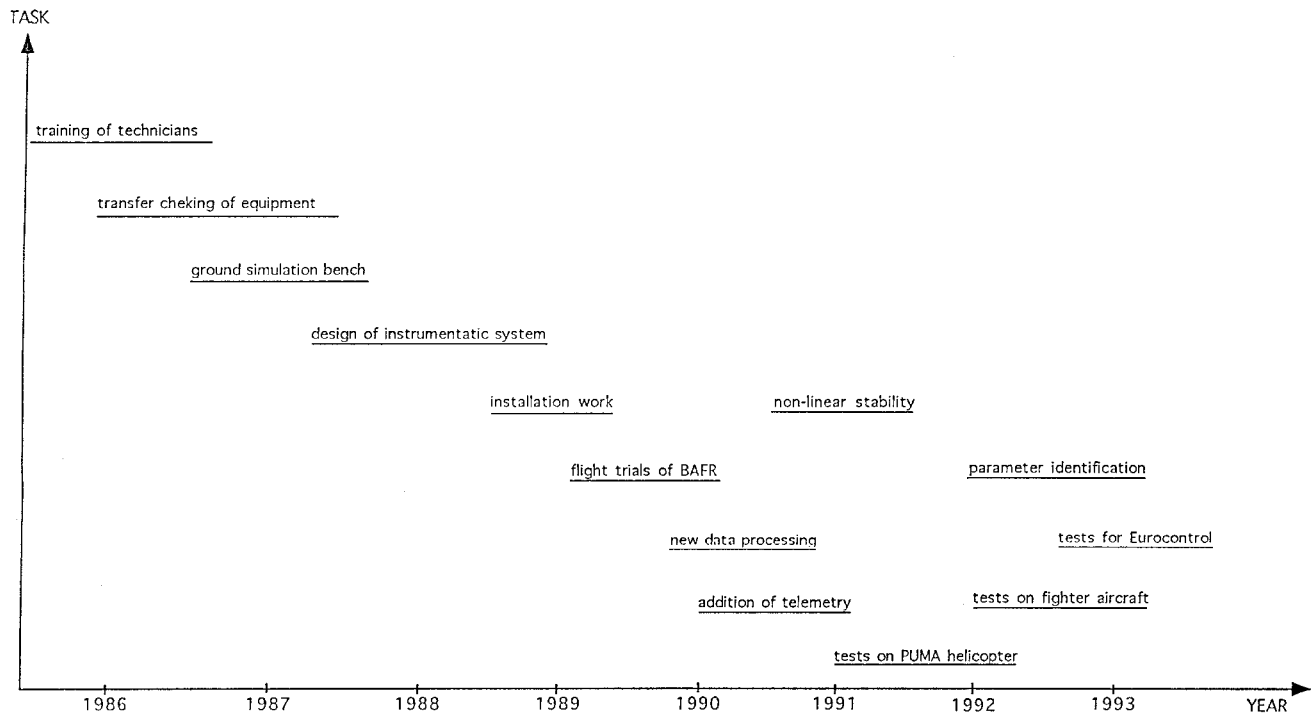

Fig. 1 Bar chart of major tasks.

arrival, and designed and set up a ground simulation bench. This work was reviewed by consultants from the institution that had donated the instrumentation. These consultants came again, on short missions, to verify the design of the flight test instrumentation system, its installation in the aircraft, and to accompany the preflight check-out and first flight tests. From then on, all operations and upgrades of the flight test facility were done locally, for example, the addition of telemetry, the updating of data recording and processing subsystems, the use of the flight test aircraft for fundamental and applied research, and the development of flight test packages for other aircraft. There was only one more consultant mission, by a senior flight test engineer, from an organization not involved in the program, to advise on the generic development of the flight test facility.

The aircraft selected as a first platform for the flight test instrumentation was a Casa 212 Aviocar twin-turboprop (Fig. 2), which has a number of desirable features. Its moderate operating costs allow flight test hours to be accumulated with modest expense, and reduces the hidden cost of downtime for modification. The aircraft has the volume to accommodate all of the instrumentation, and since it is not pressurized and does not fly at high speed, the installation of sensors and other equipment is simplified. The margins on payload and power generation, with optional equipment fitted, were adequate to cope with the flight test instrumentation system. The aircraft was well fitted with off-the-shelf equipment, including Inertial Navigation System (INS), radar altimeter, Doppler radar, autopilot, and Instrument Landing System (ILS), providing usable data sources, and using methods of extraction of signals, with no risk of corrupting the original information. The wealth of optional equipment on the aircraft did, in some cases, limit the choices of how to install flight test equipment, to avoid undesirable interferences. The flight test instrumentation installed (Fig. 3) included synchros to measure the positions of all control and high-lift surfaces, through frangible links, designed to break rather than jam in case of failure; strain gauge amplifier units (SAU) linked to the engine mounts (SAU 1 and 2) to measure engine thrust, and linked to the control column and rudder pedals (SAU 3) to measure pilot inputs; and a rack near the c.g. with rate gyros and accelerometers, to measure all components of linear and angular accelerations, independently from the INS.

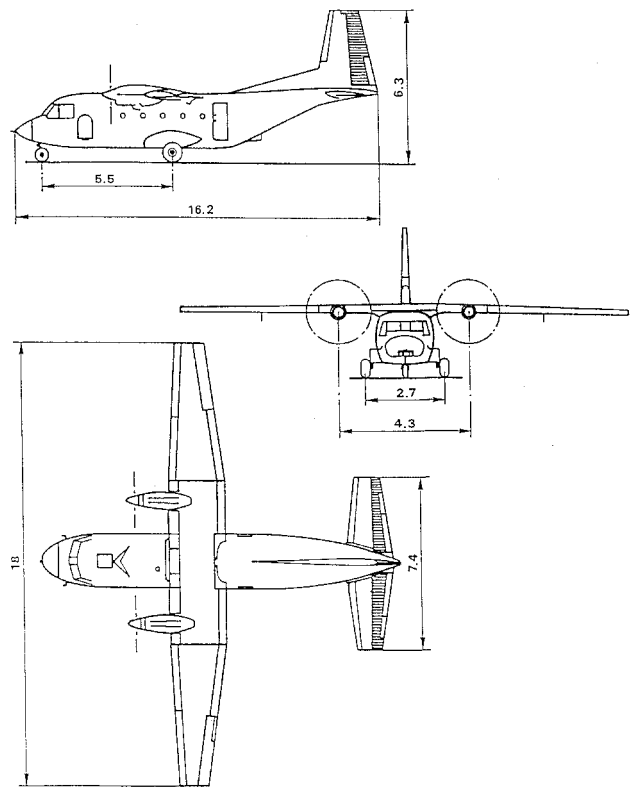

Fig. 2 Three views of the CASA 212 Aviocar.

The architecture of the flight test instrumentation system is modular, with three levels:

1) The sensors, for example, synchros, strain gauges, gyros, accelerometers, and navigation data pick-offs, are installed at the most convenient measuring positions.

2) These sensors are permanently wired to regional connector panels, one on each wing, and two in the fuselage, forward and aft.

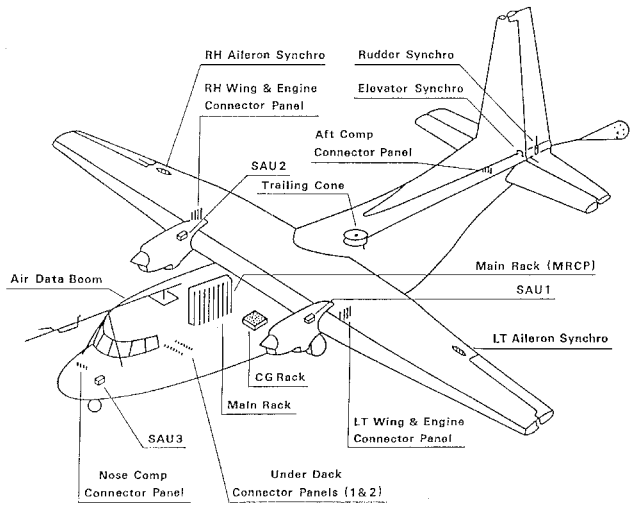

Fig. 3 Location of sensors in BAFR.

3) The regional connector panels are wired to the central connector panel, colocated with the main rack, which houses all signal conditioning and recording equipment.

This modular multilevel architecture allows simple modifications, additions or upgrades of the flight test instrumentation system. For example, additional sensors require only their local installation and wiring to the nearest regional connector panel, which has spare capacity and links to the central connector panel. The latter is a part of the main rack (Fig. 4), which, in its original form, includes signal conditioning units (SCU 1, 2, and 3), a syncho to digital conversion unit (SCDU), a power distribution unit (PDU), a digital conversion unit (DCU), and a pulse code modulation system (PCM) prior to recording on a 14-track magnetic tape. The main rack was also modified several times, without changing the sensors or other systems, for example, when adding a digital cassette to the analogue tape recording capability. Other changes involved both sensors and the main rack, for example, the addition of a telemetry capability required streaming the data flow between the onboard recorders and the transmission to the ground via dedicated antennas, installed above and below the fuselage.

The Casa 212 Aviocar was not dedicated full time to its role as basic aircraft for flight research (BAFR). Its primary mission remained that of aerial photography, requiring quick conversion to and from the flight test role. The solution to this requirement has four aspects:

1) The sensors, which would require lengthy recalibration after removal or installation, are left permanently installed, in a way that does not interfere with normal operations.

2) Likewise, the wiring between sensors and regional and central connector panels, including spare capacity, can be left permanently installed.

3) All of the signal conditioning, data processing, and recording equipment are installed in the main rack, which can be installed and removed in one day.

4) The only sensors that are removable are those on the air data boom, which can be attached and removed in the same day as the main rack.

Thus, conversion of the Casa 212 Aviocar from normal operations to the BAFR role or vice versa, takes one day only. The flight test instrumentation system on the BAFR measures 72 parameters, of a wide variety of types, including flight data, engine parameters, control and high-lift surface deflections, aircraft attitude and rates, navigation data, and strain gauge measurements. Although the total number of parameters is not large, by modern standards, the important point is the wide variety of sensors, giving a comprehensive experience in installation, design, signal conditioning, and data processing.

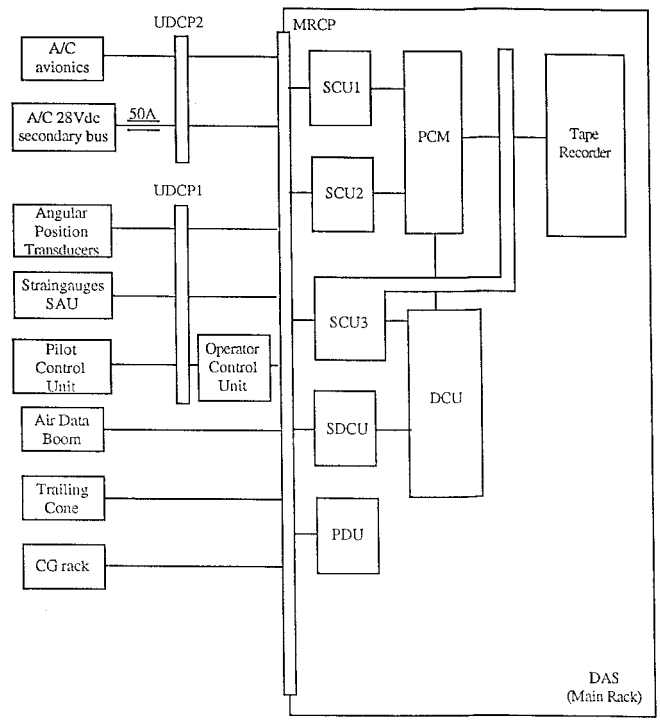

Fig. 4 Block diagram of data acquisition system.

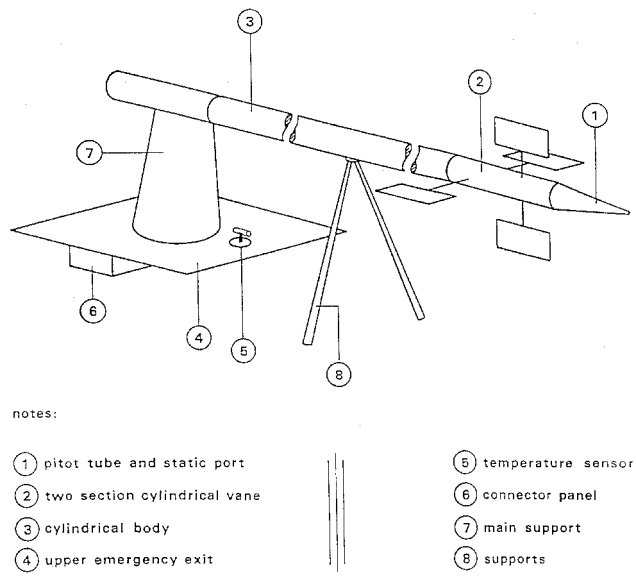

Fig. 5 Sketch of flight data boom.

The design of the air data boom (Fig. 5) is a good example of the compromise between measurement accuracy and structural ridigity and the constraints on location and removability. The location above the fuselage was decided by exclusion of other possibilities:

1) On the nose, the boom support structure would interfere with the weather radar.

2) Below the nose it would interfere with the weather or Doppler radar radiation pattern.

3) On the fuselage side, interference with the propeller slipstream would be excessive.

4) On the wing outboard of the propeller disc, misalignment because of wing bending would be excessive.

The air data boom over the fuselage needs to be relatively long to avoid excessive aerodynamic interference from the nose; a long boom would have its resonances excited by atmospheric turbulence, needing an inverted-V support on the

fuselage nose. This support has little effect on aircraft aerodynamics or crew visibility. It is removed together with the boom, using three attachment points, two on the sides of the nose and one on the top of the fuselage. The air data boom has pressure and temperature sensors and wind vanes for angle of attack and sideslip. The air data boom is just one part of the flight test instrumentation system in the BAFR, whose design and installation involved over 1000 pages of documentation, 4 km of cabling, and 7000 man-hours of work.

That experience was valuable in the subsequent design and installation of smaller, tailored flight test packages for other aircraft, for example: 1) for the measurement of wing loads resulting from a new external store for the Fiat G.91, 2) for assessment of hover performance of an Aerospatiale Puma helicopter over rough seas, 3) for prediction of the structural life of the LTV A-7P Corsair II ground attack fighters in low-level flying, 4) for measurement of structural loads on Lockheed P-3P Orion maritime patrol aircraft, and 5) for integration of a new external pod on Alpha Jet single-seat light support fighters. This work for the Portuguese Air Force involved, in some cases like 3, international cooperation, extending, in other instances like 4 to instrumenting the same type of aircraft from more than one Air Force, in a joint pooling of data. Other projects were started on an international footing:

1) European Flight Experiments into Four-Dimensional Approach and Landing (EFEDAL) is an on-going project financed by Eurocontol and involves flying real aircraft in a simulated air traffic control (ATC) scenario, to test new techniques of air traffic management (ATM), including scheduling traffic flow to achieve a 4-s precision on time of touchdown, to maximize runway usage and airport capacity.

2) Further trials in preparation of a high-frequency air-to-ground data link for automatic dependent surveillance (ADS) functions, and of satellite navigation.

3) The latter work relates to another project, under the tripartite agreement between Eurocontrol–European Space Agency–European Union, concerning the development, tests and validation of elements of a Global Navigation Satellite System (GNSS), using global positioning system/Glonass signals, with augmentation by transponders in other satellites, and differential corrections and other monitoring functions performed by ground stations. This European Geostationary Navigation Overlay Service activity is parallel to and complements the Federal Aviation Administration's Wide Area Augmentation System program.

We mention next some of the research activities, which were started in advance of availability of the aircraft, i.e., in parallel with the design of the flight test instrumentation system; in this way, as soon as the installation of the latter was completed, it was possible to implement both practical application and fundamental research programs. In connection with research activities, areas of current interest have been addressed:

1) Concerning flight in perturbed atmospheres,[1–3] a disturbance intensity indicator[4] has been applied to the aerodynamic[5] and flight[6,7] data.

2) Concerning aircraft stability,[8–10] nonlinear[11,12] and unsteady[13–15] theories have been developed, and compared with flight test data.[16–19]

3) The more conventional approach to linear, steady-state airplane stability, using Laplace transforms,[20] has also been used, and part of our results are reported here.

We start from the longitudinal dynamical equations of motion for a propeller-driven aircraft, including the effects of propeller slipstream and wing downwash on tail (Sec. II), leading to a 3×5 or 3×7 system of equations that can be reduced to a 4×4 autonomous system of equations (Sec. III). We use flight test data for the identification of parameters of the model, using test maneuvers with significant input in the frequency ranges of higher response, and their reconstruction serves as validation of the model (Sec. IV). Limitations on space prevent us from going further into the development of pitch and altitude control systems, effective within the controllability limits of the airplane. We hope that this brief selection of practical and research topics will show that a low-cost and versatile flight test platform still has a role to play in the modern, complex aerospace world.

II. Mathematical Model Including Propeller Effects

In the equations of rigid body dynamics,[21–23] applied to airplane linear stability,[8–10] the transverse and longitudinal motions decouple, and the latter are specified by variations in longitudinal F_x and normal F_z force, and pitching moment M_y:

$$Y_i \equiv \{\Delta F_x, \Delta F_z, \Delta M_y\} \qquad i = 1, 2, 3 \tag{1}$$

The independent variables would normally be the variations in longitudinal U, normal W velocity, and in pitch angle θ

$$X_j = \{\Delta U, \Delta W, \Delta W', \Delta\theta, \Delta\theta'\} \qquad j = 1, 2, 3, 4, 5 \tag{2}$$

but for a propeller-driven airplane, adequate modeling of slipstream effects also requires the time derivatives of the latter two $W' \equiv \mathrm{d}W/\mathrm{d}t$ and $\theta' \equiv \mathrm{d}\theta/\mathrm{d}t$.

If we take for reference state, straight, and level flight at U_0

$$U(t) = U_0 + u(t) \tag{3a}$$

$$W(t) = w(t) \tag{3b}$$

the vertical velocity is related to α

$$W = U_0 \Delta\alpha \tag{4a}$$

$$W' = U_0 \Delta\alpha' \tag{4b}$$

and likewise, for time derivatives [Eq. (4b)], so that

$$X_j = \{\Delta u, \Delta\alpha, \Delta\alpha', \Delta\theta, \Delta\theta'\} \tag{5}$$

is the state vector, with the five independent variables.

Turning now to the dependent variables, i.e., $\boldsymbol{M}$ and $\boldsymbol{F}$, we consider[21–23]

$$\boldsymbol{F} = m(\boldsymbol{u}' + \boldsymbol{\Omega} \wedge \boldsymbol{U}) \tag{6}$$

including the acceleration caused by translation and rotation:

$$\boldsymbol{U} = U_0 \boldsymbol{e}_x \tag{7a}$$

$$\boldsymbol{\Omega} = q\boldsymbol{e}_y \tag{7b}$$

$$\boldsymbol{u}' = u'\boldsymbol{e}_x + w'\boldsymbol{e}_y \tag{7c}$$

Thus, the longitudinal (8a) and normal (8b) components of force are given by

$$F_x = mu' \tag{8a}$$

$$F_y = m(w' - U_0 q) \tag{8b}$$

Concerning the rotation, we write L_k in terms of Ω_k and I_k:

$$\{L_x, L_y, L_z\} = \{I_x\Omega_x, I_y\Omega_y, I_z\Omega_z\} \tag{9}$$

and note, on account of Eq. (7b), that only pitching inertia is relevant here

$$\boldsymbol{L} = Iyq\boldsymbol{e}_y \tag{10}$$

The Euler equation for the moment of forces

$$\boldsymbol{M} = \boldsymbol{L}' + \boldsymbol{\Omega} \wedge \boldsymbol{L} = Iyq'\boldsymbol{e}_y \tag{11}$$

specifies the third dependent variable in Eq. (1), viz.,

$$\boldsymbol{Y}_i = \{mu',\ m(w' - U_0 q),\ Iyq'\} \tag{12}$$

with the other two coming from Eqs. (8a) and (8b).

The basic empirical assumption of stability theory is a linear relation between independent [Eq. (5)] and dependent [Eq. (12)] variables:

$$\boldsymbol{Y}_i = \sum_{j=1}^{5} A_{ij}\boldsymbol{X}_j + \boldsymbol{B}_i\delta_e \tag{13}$$

where

$$A_{ij} \equiv \frac{\partial \boldsymbol{Y}_i}{\partial \boldsymbol{X}_j} \tag{14a}$$

$$\boldsymbol{B}_i \equiv \frac{\partial \boldsymbol{Y}_i}{\partial \delta_e} \tag{14b}$$

and the control vector $\boldsymbol{B}_i$ [Eq. (14b)] relates to δ_e. The three components of the control vector

$$\boldsymbol{B}_i \equiv \left\{\frac{\partial F_x}{\partial \delta_e}, \frac{\partial F_z}{\partial \delta_e}, \frac{\partial M_y}{\partial \delta_e}\right\} \tag{15}$$

have to be identified from flight test data, as well as 12 linear stability derivatives

$$A_{i1} \equiv \frac{\partial \boldsymbol{Y}_i}{\partial u} \tag{16a}$$

$$A_{i2} \equiv \frac{\partial \boldsymbol{Y}_i}{\partial(\Delta\alpha)} \tag{16b}$$

$$A_{i3} \equiv \frac{\partial \boldsymbol{Y}_i}{\partial(\Delta\alpha')} \tag{16c}$$

$$A_{i5} \equiv \frac{\partial \boldsymbol{Y}_i}{\partial(\Delta\theta')} \tag{16d}$$

the remaining three components A_{i4} of the 15 elements of the stability matrix, can be calculated from the longitudinal and normal components of weight:

$$G_x = -mg\sin\theta \tag{17a}$$

$$G_z = mg\cos\theta \tag{17b}$$

which are the only dependent variables influenced by θ:

$$A_{14} = \frac{\partial F_x}{\partial\theta} = \frac{\partial G_x}{\partial\theta} = -mg\cos\theta \tag{18a}$$

$$A_{24} = \frac{\partial F_z}{\partial\theta} = \frac{\partial G_z}{\partial\theta} = -mg\sin\theta \tag{18b}$$

$$A_{34} = \frac{\partial M_y}{\partial\theta} = 0 \tag{18c}$$

Thus, the mathematical model of linear longitudinal stability [Eq. (13)], has 15 parameters to be determined [Eqs. (15) and (16a–16d)].

We can write the system in dimensionless form, starting with the five independent variables [Eq. (5)], using U_0 and c

$$\bar{\boldsymbol{X}}_j = \{u/U_0,\ \Delta\alpha,\ c\Delta\alpha'/U_0,\ \Delta\theta,\ c\Delta\theta'/U_0\} \tag{19}$$

concerning the dependent variables [Eq. (1)], forces are made dimensionless dividing by dynamic pressure $\frac{1}{2}\rho U_0^2$ times S

$$\bar{\boldsymbol{Y}}_i = \{2F_x/\rho U_0^2 S,\ 2F_z/\rho U_0^2 S,\ 2M_y/\rho U_0^2 Sc\} \tag{20}$$

and for the moment we use the chord as well.

The linear longitudinal stability system [Eq. (13)] now becomes

$$\begin{bmatrix} D_1 \\ D_2 \\ D_3 \end{bmatrix} \delta_e = \begin{bmatrix} -C_{11} & -C_{12} & -C_{13} & -C_{14} & -C_{15} & \mu & 0 \\ -C_{21} & -C_{22} & \mu - C_{23} & -C_{24} & -\mu - C_{25} & 0 & 0 \\ -C_{31} & -C_{32} & -C_{33} & -C_{34} & -C_{35} & 0 & \nu \end{bmatrix} \times \begin{matrix} u/U_0 \\ \Delta\alpha \\ c\Delta\alpha'/U_0 \\ \Delta\theta \\ c\Delta\theta'/U_0 \\ u'c/U_0^2 \\ c^2\Delta\theta''/U_0^2 \end{matrix} \tag{21}$$

where: 1) the $\boldsymbol{D}_i$ relate the dimensionless forces and moments [Eq. (20)] to elevator deflection:

$$\{D_1, D_2, D_3\} = \left(\frac{2}{\rho U_0^2 S}\right)\left\{\frac{\partial F_x}{\partial\delta_e}, \frac{\partial F_z}{\partial\delta_e}, c^{-1}\frac{\partial M_y}{\partial\delta_e}\right\} \tag{22}$$

2) we have made m and I_y dimensionless by introducing μ and ν

$$\mu = 2m/\rho Sc \tag{23a}$$

$$\nu \equiv 2I_y/\rho Sc^3 \tag{23b}$$

3) of the coefficients C_{ij}, three equations [Eqs. (18a–18c)] are determined a priori

$$\{C_{14}, C_{24}, C_{34}\} = j\{\cos\theta, \sin\theta, 0\} \tag{24a}$$

$$j \equiv 2mg/\rho U_0^2 S = \mu gc/U_0^2 \tag{24b}$$

where we introduce j; 4) the remaining 12 coefficients involve stability derivatives

$$\begin{aligned} C_{11} &\equiv \left(\frac{2}{\rho U_0 S}\right)\frac{\partial F_x}{\partial u} \quad C_{12} \equiv \left(\frac{2}{\rho U_0^2 S}\right)\frac{\partial F_x}{\partial(\Delta\alpha)} \\ C_{13} &\equiv \left(\frac{2c}{\rho U_0^3 S}\right)\frac{\partial F_x}{\partial(\Delta\alpha')} \quad C_{15} \equiv \left(\frac{2c}{\rho U_0^3 S}\right)\frac{\partial F_x}{\partial(\Delta\theta')} \\ C_{21} &\equiv \left(\frac{2}{\rho U_0 S}\right)\frac{\partial F_z}{\partial u} \quad C_{22} \equiv \left(\frac{2}{\rho U_0^2 S}\right)\frac{\partial F_z}{\partial(\Delta\alpha)} \\ C_{23} &\equiv \left(\frac{2c}{\rho U_0^3 S}\right)\frac{\partial F_z}{\partial(\Delta\alpha')} \quad C_{25} \equiv \left(\frac{2c}{\rho U_0^3 S}\right)\frac{\partial F_z}{\partial(\Delta\theta')} \\ C_{31} &\equiv \left(\frac{2}{\rho U_0 Sc}\right)\frac{\partial M_y}{\partial u} \quad C_{32} \equiv \left(\frac{2}{\rho U_0^2 Sc}\right)\frac{\partial M_y}{\partial(\Delta\alpha)} \\ C_{33} &\equiv \left(\frac{2}{\rho U_0^3 S}\right)\frac{\partial M_y}{\partial(\Delta\alpha')} \quad C_{35} \equiv \left(\frac{2}{\rho U_0^3 S}\right)\frac{\partial M_y}{\partial(\Delta\theta')} \end{aligned} \tag{25}$$

to be identified from flight tests.

III. Frequency and Damping of Longitudinal Modes

The system [Eq. (21)] appears as a 3×7 matrix, but it can be written as a 4×4 autonomous system of ordinary differential equations (ODEs).[24–26] For this purpose we choose as

independent variables u, $\Delta\alpha$, $\Delta\theta$, and the pitch rate or angular velocity in pitch $q \equiv \Delta\theta'$:

$$\boldsymbol{Z}_i = \{u,\ \Delta\alpha,\ \Delta\theta,\ q\} \qquad i = 1,\ 2,\ 3,\ 4 \tag{26}$$

The autonomous system specifies the time rates of the variables as linear functions of the variables

$$Z_i' = \sum_{j=1}^{4} H_{ij} Z_j + \boldsymbol{N}_i \delta_e \tag{27}$$

where 1) because $q = \Delta\theta'$, one row of the matrix H_{ij} is a unit vector

$$H_{31} = H_{32} = H_{33} = 0 = N_3, \quad H_{34} = 1 \tag{28}$$

and one component of $\boldsymbol{N}_i$ as well; 2) the remaining components of the vector $\boldsymbol{N}_i$ are

$$N_1 \equiv (U_0^2/c)\{D_2 C_{13} + D_1(\mu - C_{23})\}/\{\mu(\mu - C_{23})\} \tag{29a}$$

$$N_2 \equiv (U/c) D_2/(\mu - C_{23}) \tag{29b}$$

$$N_3 \equiv (U_0/c)^2\{D_2 C_{33} + D_3(\mu - C_{23})\}/\nu \tag{29c}$$

3) the remaining components of H_{ij} are

$$\mu(\mu - C_{23})\{H_{11}, H_{12}, H_{13}, H_{14}\} = \{(U_0/c)[C_{13}C_{21} + C_{11}(\mu - C_{23})], (U_0^2/c)[C_{13}C_{22} + C_{12}(\mu - C_{23})], (U_0^2/c)[-C_{13}C_{24} - C_{14}(\mu - C_{23})], U_0[C_{13}(\mu + C_{25}) + C_{15}(\mu - C_{23})]\} \tag{30a}$$

$$(\mu - C_{23})\{H_{21}, H_{22}, H_{23}, H_{24}\} = \{C_{21}/c, (U_0/c)C_{22}, -(U_0/c)C_{24}, -C_{25} + \mu\} \tag{30b}$$

$$j(\mu - C_{23})\{H_{41}, H_{42}, H_{43}, H_{54}\} = \{(c^2/U_0^3) \times [C_{33}, C_{21} + C_{31}(\mu - C_{23})], (c/U_0)^2[C_{33}, C_{22} + C_{32}(\mu - C_{23})], (c/U_0)^2 C_{33}, C_{24}, (c/U_0)[C_{33}(C_{25} + \mu) + C_{35} + (\mu - C_{23})]\} \tag{30c}$$

The values of the parameters for our aircraft are as follows: $m = 6 \times 10^3$ kg, $I_y = 4.4 \times 10^5$ kg m^2, $S = 40$ m^2, $c = 2.13$ m, $U_0 = 130$ kn (=66.9 m/s), $g = 9.8$ m s^{-2}, $h = 3.048$ m, $\rho = 0.905$ kg m^{-3}, $C_L = 0.724$, $C_b = 0.059$, $p \equiv \frac{1}{2}\rho U_0^2$ (=2025 N m^{-2}), $\mu = 155.6$, $\nu = 251.6$, and $j = 0.726$. And from these we obtain the matrix C_{ij} and vector $\boldsymbol{D}_i$ in Table 1, which, in turn, specify the matrix H_{ij} and vector $\boldsymbol{N}_i$

$$H_{ij} = \begin{bmatrix} -0.024 & 0.216 & -0.334 & 0 \\ -0.129 & -1.16 & 0 & 0.987 \\ 0 & 0 & 0 & 1 \\ 0.0229 & -2.928 & 0 & -0.709 \end{bmatrix} \tag{31a}$$

$$\boldsymbol{N}_i = \begin{bmatrix} 0 \\ -0.0576 \\ 0 \\ -2.796 \end{bmatrix} \tag{31b}$$

in the system [Eq. (27)]. These data were obtained from a collaborative parameter identification work between DLR and Instituto Nacional de Tecnologias Aerospaciales (INTA, Spain). It was used as an initial estimate in our parameter identification work, in a procedure that consisted of the following steps:

1) Obtaining Bode diagrams, to determine the frequency ranges allowing higher accuracy in the identification of parameters.

Table 1 Stability and control derivatives

Matrix	Vector
$C_{11} = -0.118$	$\boldsymbol{D}_1 = 0.0$
$C_{12} = 0.469$	$\boldsymbol{D}_2 = -0.284$
$C_{13} = 0.0$	$\boldsymbol{D}_3 = -0.71$
$C_{15} = 0.0$	——
$C_{21} = -1.779$	——
$C_{22} = -5.721$	——
$C_{23} = -2.26$	——
$C_{25} = -6.78$	——
$C_{31} = 0.0$	——
$C_{32} = -0.793$	——
$C_{33} = -5.66$	——
$C_{35} = 0.0$	——

2) Designing control schedules, whose spectra have larger amplitude in these frequency ranges, to be used as inputs for flight tests.

3) Sampling the flight test data, and using a parameter identification routine, to obtain the parameters of the mathematical model.

4) Using the mathematical model, with these parameters, to reconstruct the flight maneuvers flown, and compare with flight data records, as a validation. The validated mathematical model was used to design control systems, for pitch and altitude, taking into account the full fourth-order control system, with short-period and phugoid modes, or a reduced second-order system. Since we have no space to detail all of this work here, we conclude with a discussion of the two longitudinal modes, from the data given before.

Since we have a linear autonomous system of ODEs with constant parameters, it is convenient to use the Laplace transform[27–29]

$$\tilde{Z}_i(s) = \int_0^\infty \boldsymbol{Z}_i(t) e^{-st}\, \mathrm{d}t \tag{32}$$

which leads from the system of differential equations (27), to a linear algebraic system of equations:

$$\boldsymbol{Z}_i(0) - s\tilde{Z}_i(s) = \sum_{j=1}^{4} H_{ij}\tilde{Z}_j(s) + s^{-1}\boldsymbol{N}_i\delta_e \tag{33}$$

In the absence of control inputs or initial disturbances, the system is homogeneous

$$\delta_e = 0 = \boldsymbol{Z}_i(0) \qquad \sum_{j=1}^{4} (H_{ij} + s\delta_{ij})\tilde{Z}_j(s) = 0 \tag{34}$$

where we have introduced the identity matrix

$$\delta_{ij} = \begin{cases} 0 & \text{if} \quad i \neq j \\ 1 & \text{if} \quad i = j \end{cases} \tag{35}$$

The system (34) has a nontrivial solution

$$\{\tilde{Z}_i(s), \tilde{Z}_2(s), \tilde{Z}_3(s), \tilde{Z}_4(s)\} \neq \{0, 0, 0, 0\} \tag{36}$$

if and only if the determinant of coefficients vanishes

$$0 = \mathrm{Det}(H_{ij} + s\delta_{ij}) = \sum_{n=0}^{4} a_n s^n \tag{37}$$

leading to a polynomial of the fourth-degree, with coefficients

$$a_n = 0.00637,\ 0.00527,\ 0.179,\ 0.0895,\ 0.0473 \qquad n = 0,\ 1,\ 2,\ 3,\ 4 \tag{38}$$

Note that $-s$ are the eigenvalues of H_{ij} [Eq. (31a)], and, hence, the roots of Eqs. (37) and (38).

The polynomial (37) may be factorized

$$0 = a_4(s^2 + 2\xi_{ph}\omega_{ph}s + \omega_{ph}^2)(s^2 + 2\xi_{sp}\omega_{sp}s + \omega_{sp}^2) \quad (39)$$

emphasizing the ξ and ω of the phugoid and short-period modes.[30–32] In the present case (Fig. 6), the phugoid has frequency

$$\omega_{ph} = 0.191 \text{ s}^{-1} \quad (40a)$$

and period

$$\tau_{ph} = 2\pi/\omega_{ph} = 32.8 \text{ s} \quad (40b)$$

and damping

$$\xi_{ph} = 0.0314 \quad (41a)$$

and decay time

$$\lambda_{ph} = 0.693/\omega\xi = 116 \text{ s} \quad (41b)$$

where the latter is the time for the amplitude to decay to half the initial value. The frequency and period are one order of magnitude apart from those of the short-period mode:

$$\omega_{sp} = 1.903 \text{ s}^{-1} \quad (42a)$$

$$\tau_{sp} = 3.30 \text{ s} \quad (42b)$$

and the damping and decay time

$$\xi_{sp} = 0.467 \text{ s}^{-1} \quad (43a)$$

$$\lambda_{sp} = 0.780 \text{ s} \quad (43b)$$

show even greater contrast.

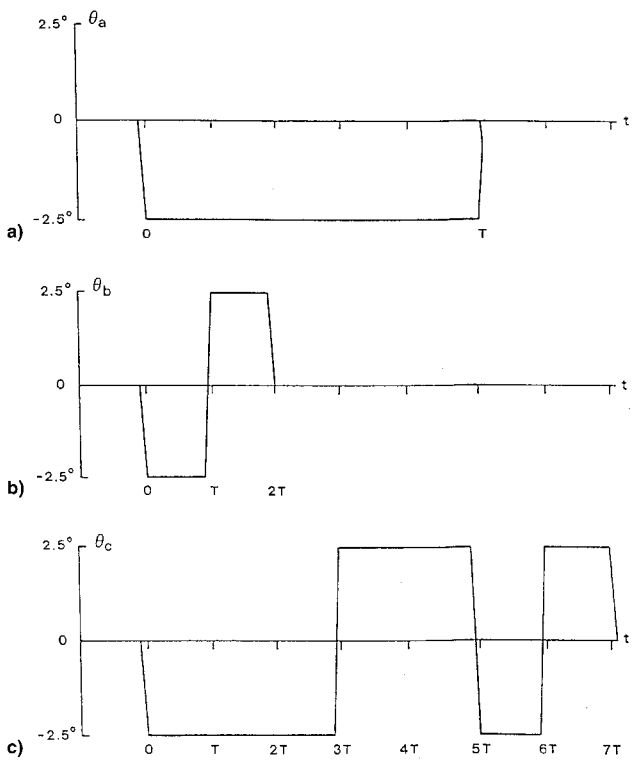

Fig. 6 a) Set, b) doublet, and c) 3211 imputs.

IV. Comparison with Flight Test Results

The parameters used in the longitudinal stability model of the aircraft (Secs. II and III), were obtained from flight test records of chosen maneuvers, performed on our Casa 212 Aviocar (Fig. 2) modified test aircraft. Three candidate pitch inputs were considered, as shown in Fig. 6, namely a step (Fig. 6a), doublet (Fig. 6b), and 3211 (Fig. 6c). The signals have a common amplitude of -2.5 deg, the same as in the earlier DLR/INTA parameter identification work,[33] which we used as initial data.

The next choice was T, and three values were considered: $T = 0.6$, 1.0, and 1.5 s. The step input (Fig. 6a) led to a P vs

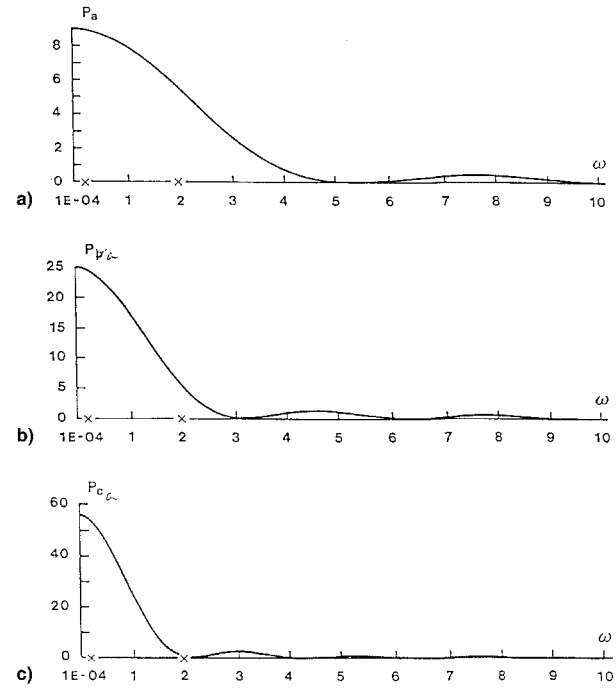

Fig. 7 P vs ω of step inputs of duration T = a) 0.6, b) 1.0, and c) 1.5 s.

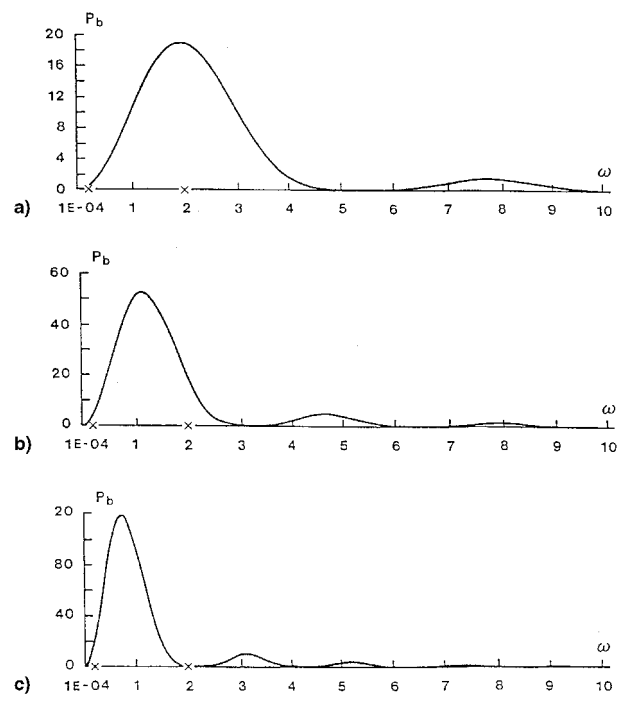

Fig. 8 P vs ω for doublet input of duration T = a) 0.6, b) 1.0, and c) 1.5 s.

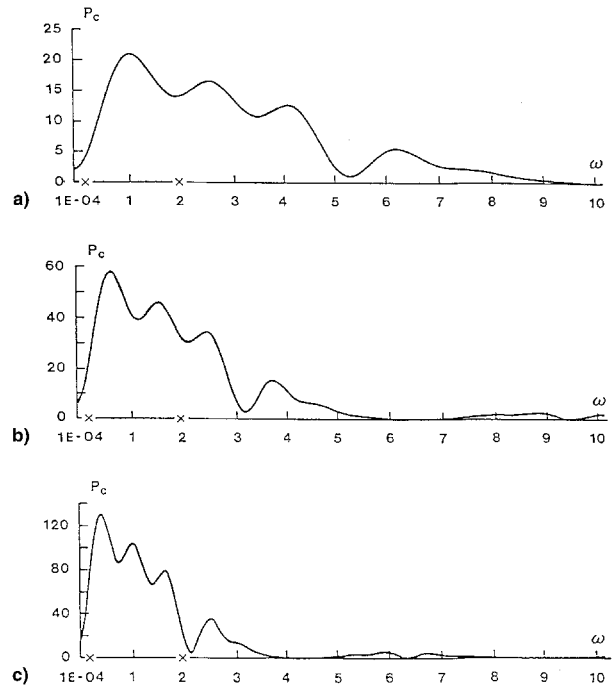

Fig. 9 *P* vs ω for 3211-input of duration T = a) 0.6, b) 1.0, and c) 1.5 s.

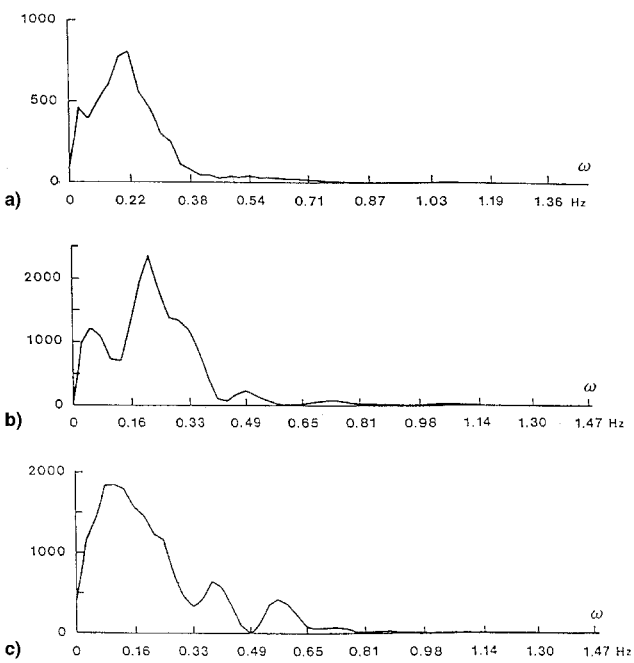

Fig. 10 *P* vs ω in Hz for maneuvers a) A, b) B, and c) C.

ω in Fig. 7; the power decays monotonically (apart from small secondary humps), and is more concentrated at lower frequencies for longer input durations. This is a typical property of Fourier transforms[34–40] that a longer signal has a narrower spectrum. The doublet input (Fig. 6b) has peak power (Fig. 8) at a frequency that reduces with the duration of the pulse, and again becomes narrower for longer pulses, while retaining small secondary humps. The advantage of the 3211 input (Fig. 6c) is seen in the much broader power spectrum (Fig. 9), with four noticeable peaks and three valleys in between, the last being deeper; again the power spectrum is narrower for longer inputs and secondary humps are negligible.

The power spectra for the preceding inputs can be calculated analytically. The power spectrum (44a) is the square of the modulus of the Fourier transform (44b) of the pitch input:

$$P(\omega) \equiv |f(\omega)|^2 \tag{44a}$$

$$f(\omega) \equiv \int_{-\infty}^{+\infty} \theta(t) e^{i\omega t}\, d\omega \tag{44b}$$

where in Eq. (44b) we omit the factor $1/2\pi$ (or $1/\sqrt{2\pi}$, depending on the reference[34–38]). Using the definition of unit function[39–44]

$$H(t) \equiv \begin{cases} 0 & \text{if} \quad t < 0 \\ 1 & \text{if} \quad t > 0 \end{cases} \tag{45}$$

we can specify step (46a), doublet (46b), and 3211 (46c) inputs

$$\theta_a(t) = \theta_0[H(t) - H(t - T)] \tag{46a}$$

$$\theta_b(t) = \theta_0[H(t) - 2H(t - T) + H(t - 2T)] \tag{46b}$$

$$\theta_c(t) = \theta_0[H(t) - 2H(t - 3T) + 2H(t - 5T) - 2H(t - 6T) + H(t - 7T)] \tag{46c}$$

all with the same amplitude θ_0, viz., $\theta_0 = -2.5$ deg in Fig. 10.

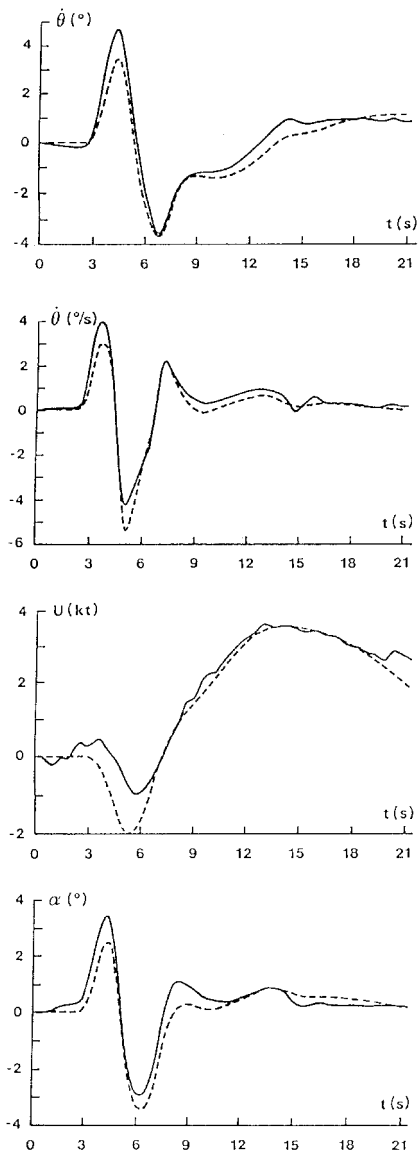

Fig. 11 Pitch in degrees, pitch rate in degrees per second, airspeed in knots, and angle-of-attack in degrees, vs time in seconds, for maneuver A, as flown (solid line) and as reconstructed by stability model (dashed line).

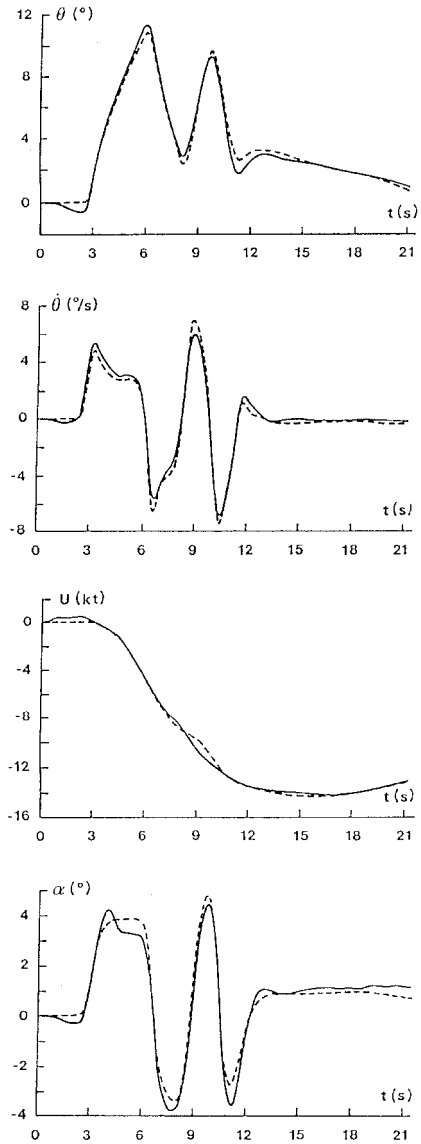

Fig. 12 Pitch in degrees, pitch rate in degrees per second, airspeed in knots, and angle-of-attack in degrees, vs time in seconds, for maneuver B, as flown (solid line) and as reconstructed by stability model (dashed line).

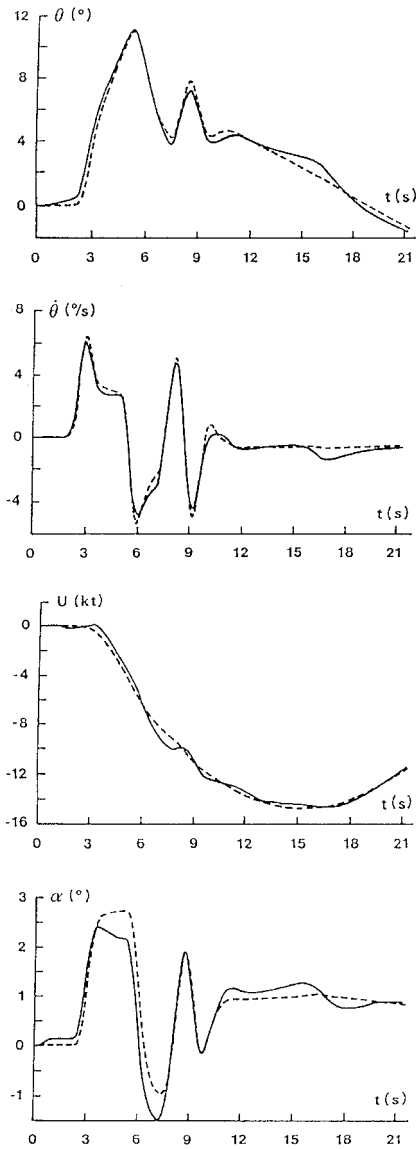

Fig. 13 Pitch in degrees, pitch rate in degrees per second, airspeed in knots, and angle-of-attack in degrees, vs time in seconds, for maneuver C, as flown (solid line) and as reconstructed by stability model (dashed line).

Substitution of Eqs. (46a–46c) in Eq. (44b), and the use of Eq. (45), specifies:

$$f_a(\omega) = i(\theta_0/\omega)(1 - e^{i\omega T}) \tag{47a}$$

$$f_b(\omega) = i(\theta_0/\omega)(1 - 2e^{i\omega T} + e^{i2\omega T}) \tag{47b}$$

$$f_c(\omega) = i(\theta_0/\omega)(1 - 2e^{i3\omega T} + e^{i5\omega T} - 2e^{i6\omega T} + e^{i7\omega T}) \tag{47c}$$

respectively, the spectra of step (47a), doublet (47b), and 3211 (47c) inputs. The modulus square (44a) specifies, respectively,

$$P_a(\omega) = 2(\theta_0/\omega)^2[1 - \cos(\omega T)] \tag{48a}$$

$$P_b(\omega) = 2(\theta_0/\omega)^2[3 - 4\cos(\omega T) - \cos(2\omega T)] \tag{48b}$$

$$P_c(\omega) = 2(\theta_0/\omega)^2[7 - 6\cos(\omega T) - 4\cos(2\omega T) + 6\cos(3\omega T) - 4\cos(4\omega T) + 2\cos(5\omega T) - 2\cos(6\omega T) + \cos(7\omega T)] \tag{48c}$$

the power spectra of step (48a), doublet (48b), and 3211 (48c) inputs.

Three examples of power spectra of pitch maneuvers actually flown, are shown in Fig. 10, viz., a doublet for maneuver A and two examples of 32AA for maneuvers B and C. The power spectra are, respectively, unimodal (Fig. 10a), bimodal (Fig. 10b), and trimodal (Fig. 10c) for maneuvers A, B, and C, respectively. The solid lines in Figs. 11, 12, and 13 show the flight records, respectively, for maneuvers A, B, C, of pitch angle (top) in degrees, pitch rate (second from top) in degrees per second, airspeed (second from bottom) in knots, and angle of attack (bottom) in degrees, vs time in seconds. It is seen that maneuver A is pitch-up followed by pitch-down, maneuver B is double pitch-up, and maneuver C is also a double pitch-up with a smaller second input.

There exists a variety of parameter identification methods,[45–48] and those used in flight testing[49–53] include linear and nonlinear methods. Since our inputs are of small amplitude, we used a linear method, the maximum likelihood method for which ready packages like Matlab and MATRIX exist.[54,55] Methods suitable for nonlinear models were used elsewhere.[7] The parameter identification of stability derivatives for the three maneuvers led to the frequencies and damping of the phugoid and short period modes indicated in Table 2, together

Table 2 Frequency and damping of phugoid and short-period modes

Result	ω_{ph}	ξ_{ph}	ω_{sp}	ξ_{sp}
Theory	0.191	0.0314	1.930	0.487
Maneuver A	0.1166	0.1067	2.2967	0.7275
Maneuver B	0.1494	0.871	2.7114	0.5885
Maneuver C	0.174	0.0759	2.3459	0.7494

with the theoretical values calculated in Sec. IV. The final validation of our linear longitudinal stability model is the reconstruction of airplane response using the model (dashed lines), and its comparison with flight records (solid lines), in Figs. 11, 12, and 13, respectively, for maneuvers A, B, and C.

Acknowledgments

The creation of an IFTF in Portugal, and the implementation of its first flying element BAFR was made possible by the generosity of institutions and devotion of individuals. AGARD, which as part of the Support Program to Southern Flank Nations, provided the key contacts and funding for international travel and local subsistence, under Projects P.45 and P.87, supported at various levels, from the Flight Test Editorial Committee through the Flight Mechanics Panel and National Delegates Board. In Holland, the National Aerospace Laboratory, which offered the flight test instrumentation, and whose management and staff supported the project: Chairman O. H. Gerlach, Director I. J. van der Bliek, the Heads of the Flight Division, H. Moelke and J. T. M. van Doorn, and the Flight Test Engineers P. Hollestelle and R. van der Welde. In Germany, G. Madelung, who arranged for the training of Portuguese engineers on flight testing with the group of G. Schanzer, at the Institut for Flugfuhrung of Braunschweig Technical University, and the DLR-Braunschweig, which offered telemetry and recording equipment, and consultations, from the group of H. Bothe. The Portuguese Air Force, which provided the aircraft and pilots (from Flight 401 at Sintra Air Base), the flight support laboratory (at the Air Force Academy), the certification requirements (mechanics–Aeronautical Materials Division and electrics–Electrotechnical Division directorates), the installation work, General Workshops for Aeronautical Material, and project staff, with support and contributions from Chief of Staff Lemos Ferreira, AGARD National Delegates F. Q. Bourbon, A. A. Portela, and G. Calvão Borges, and the Air Force Academy staff A. M. S. Cardoso and J. Lima. The National Board for Scientific, and Technological Research, which funded the Aeronautics Laboratory at the Instituto Superior Tècnico, of Lisbon Technical University. And finally thanks go to A. Benoit and J. F. Renaudie, who advised on the development of the flight test facility.

References

[1]Etkin, B., "Turbulent Wind and Its Effect on Flight," *Journal of Aircraft*, Vol. 18, No. 5, 1981, pp. 327–345.

[2]Frost, W., Cosby B., and Camp, D. W., "Flight Through Thunderstorm Outflows," *Journal of Aircraft*, Vol. 16, No. 1, 1979, pp. 11–15.

[3]Parks, E. K., Wingrove, R. C., Bach, R. E., and Mehta, R. S., "Identification of Vortex-Induced Clear Air Turbulence Using Airline Flight Records," *Journal of Aircraft*, Vol. 22, 1985, pp. 124–129.

[4]Campos, L. M. B. C., "On the Effects of Atmospheric Disturbances on Aircraft Aerodynamics," *Aeronautical Journal*, Paper 1085, June 1984, pp. 257–264.

[5]Campos, L. M. B. C., "On Aircraft Flight Performance in a Perturbed Atmosphere," *Aeronautical Journal*, Paper 1305, Oct. 1986, pp. 301–312.

[6]Campos, L. M. B. C., "On the Disturbance Intensity as an Indicator of Aircraft Performance Degradation in a Perturbed Atmosphere," *2nd International Symposium on Aviation Safety*, Cepaduès, Toulouse, France, 1986, pp. 175–190.

[7]Campos, L. M. B. C., Fonseca, A. A., and Azinheira, J. R. C., "Some Elementary Aspects of Non-Linear Airplane Speed Stability in Constrained Flight," *Progress in Aerospace Sciences*, Vol. 31, 1995, pp. 137–169.

[8]Perkins, E. W., and Hage, L., *Airplane Performance, Stability and Control*, Wiley, New York, 1956.

[9]Duncan, W. J., *Principles of Control and Stability of Aircraft*, Cambridge Univ. Press, Cambridge, England, UK, 1952.

[10]Babister, A. W., *Aircraft Dynamic Stability and Response*, Pergamon, Oxford, England, UK, 1980.

[11]Campos, L. M. B. C., and Aguiar, A. J. M. N., "On the Inverse Phugoid Problem as an Instance of Non-Linear Stability in Pitch, *Aeronautical Journal*, Paper 1559/1, Sept. 1989, pp. 241–253.

[12]Campos, L. M. B. C., "On the Compensation of the Phugoid Mode Induced by Wind Shears and Initial Conditions," 16th International Congress of the Aeronautical Sciences Congress, Jerusalem, 1988 (Paper 3.3.1).

[13]Campos, L. M. B. C., "On a Pitch Control Law for Constant Glide Slope Through Windshears and Other Disturbances," *Aeronautical Journal*, Paper 1559/2, Oct. 1989, pp. 290–300.

[14]Campos, L. M. B. C., "A Pitch Control Law for the Compensation of the Phugoid Mode Induced by Windshear," 75th FMP Symposium on Flight in Adverse Weather Conditions, CP-470, AGARD, 1989 (Paper 11).

[15]Campos, L. M. B. C., "On Non-Linear Longitudinal Stability of an Aircraft in a Dive, in the Presence of Atmospheric Disturbances," 67th Guidance and Control Panel, Symposium on Stability in Aerospace Systems (Toulouse, France), 1992.

[16]Campos, L. M. B. C., Ramos, H. F., and Fonseca, A. A., "On the Development of a Basic Flight Test Capability and Some Related Research Projects," 74th Flight Mechanics Panel Symposium on Flight Test Techniques, AGARD, 1988 (Paper 28).

[17]Campos, L. M. B. C., "Comparison of Non-Linear Pitch Stability Theory with Data from BAFR (Basic Aircraft for Flight Research)," AIAA/HHS/ASEE Aircraft Design and Operations Meeting (Seattle, WA), AIAA, Washington, DC, 1989.

[18]Campos, L. M. B. C., and Azinheira, J. R. C., "On the Development of the BAFR (Basic Aircraft for Flight Research) in Portugal," 17th International Congress of the Aeronautical Sciences Congress (Stockholm, Sweden), 1990.

[19]Campos, L. M. B. C., "On Automated Analysis of Flight Test Data," 32nd Flight Mechanics Panel Symposium on Flight Testing (Crete, Greece), 1992.

[20]Babister, A. W., *Aircraft Stability and Control*, Oxford Univ. Press, Oxford, England, UK, 1961.

[21]Whittaker, E. T., *Analytical Mechanics*, Cambridge Univ. Press, Oxford, England, UK, 1937.

[22]Sommerfeld, A., *Mechanics*, Academic, New York, 1942.

[23]Landau, L. D., and Lifshitz, E. F., *Mechanics*, Pergamon, Oxford, England, UK, 1949.

[24]Ince, E. L., *Ordinary Differential Equations*, Dover, New York, 1926.

[25]Forsyth, A. R., *Differential Equations*, MacMillan, New York, 1927.

[26]Esgolts, L., *Differential Equations and Calculus of Variations*, Mir Publishers, Moscow, 1977.

[27]Jeffreys, H. S., and Jeffreys, B. S., *Methods of Mathematical Physics*, Cambridge Univ. Press, Cambridge, England, UK, 1954.

[28]Lepage, W. R., *Complex Variables and Laplace Transform for Engineers*, McGraw–Hill, New York, 1961.

[29]Sneddon, I. N., *Integral Transforms*, McGraw–Hill, New York, 1974.

[30]Lanchester, F. W., *Aerodonetics*, Constable, London, 1907.

[31]Mises, R. V., *Theory of Flight*, Dover, New York, 1944.

[32]Etkin, B., *Dynamics of Atmospheric Flight*, McGraw–Hill, New York, 1972.

[33]"Casa C-212 Flight Test and Parameter Identification," Inst. für Flugfuhrung, DFVLR, 1976.

[34]Carslaw, H. S., *Fourier Series and Integrals*, Dover, New York, 1930.

[35]Bochner, S., *Vorlesungem Ueber die Fourierische Integral*, Chelsea Publ., 1948.

[36]Wiener, N. W., *The Fourier Integral, and Certain of Its Applications*, Cambridge Univ. Press, Cambridge, England, UK, 1933.

[37]Titchmarsch, E. C., *Theory of Fourier Integrals*, Oxford Univ. Press, Oxford, England, UK, 1948.

[38]Bracewell, R. N., *The Fourier Transform and its Applications*, McGraw–Hill, New York, 1986.

[39]Heaviside, O., *Papers*, Chelsea Publ., New York, 1986.

[40]Schwartz, L., *Les Distributions*, Hermman, Paris, 1949.
[41]Lighthill, M. J., *Fourier Analysis and Generalized Functions*, Cambridge, Univ. Press, Cambridge, England, UK, 1958.
[42]Guelfand, G., and Chilov, G., *Distribution*, Academic, New York, 1962.
[43]Jones, D. S., *Generalized Functions*, McGraw–Hill, New York, 1966.
[44]Vladimirov, L., Mir Publishers, Moscow, 1979.
[45]Ljung, L., and Soderstrom, T., *Theory and Practice of Recursive Identification*, MIT Press, Cambridge, MA, 1983.
[46]Ljung, L., *System Identification: Theory for the User*, Prentice–Hall, Englewood Cliffs, NJ, 1987.
[47]Soderstrom, T., and Stoica, P., *System Identification*, Prentice–Hall, Englewood Cliffs, NJ, 1989.
[48]Laban, M., "On-Line Aircraft Aerodynamic Model Identification," Ph.D. Dissertation, Delft Univ., Delft, The Netherlands, 1994.
[49]Mehra, R. K. and Grupta, N. K., *Status of Input Design for Aircraft Parameter Identification*, CP-172, AGARD, 1975 (Paper 12-1-21).
[50]Maine, R. E., and Illif, K. W., *Identification of Dynamic Systems*, Vol. 2, AGARD AG-300, 1985.
[51]Maine, R. E., and Illif, K. W., Identification of Dynamic Systems Applications to Aircraft. Part 1: The Output Error Approach, Vol. 3, Pt. 1, AGARD AG-300, 1986.
[52]Hamel, P. (ed.), "Rotorcraft System Identification," AGARD Advisory Rept. 280, 1991.
[53]Mulder, J. A., Sridhar, J. K., and Breeman, J. H., *Identification of Dynamic Systems-Applications to Aircraft. Part II: Nonlinear Analysis and Manouever Design*, Vol. 3, Pt. 2, AGARD AG-300, 1994.
[54]*Matrixn User Manual*, Integrated Systems Inc., CA, 1990.
[55]Ljung, L., *System Identification Toolbox User's Guide*, The Math Works, Inc., MA, 1991.